Advances in DCC N20 Stability and Calibration Methodologies

Prathana Khakurel, David Doelling, Conor Haney, Rajendra Bhatt, Arun Gopalan, Benjamin Scarino

GSICS VIS/NIR monthly web meeting, Sept 12, 2024

Background

- DCC calibration technique (DCCT), an ensemble statistical approach, first introduced by Hu et al. in 2004 for monitoring CERES instrument calibration, particularly effective for VIS and NIR bands
- Doelling et al. 2011 (GSICS ATBD) and 2013 used the Hu BRDF and PDF mode statistic to monitor the stability of visible imagers
  - Noted that the DCC reflectivity varied across the tropics for all bands
- Multiple VIS-NIR sensitivity studies from the calibration community
  - Median, inflection point statistics
  - footprint size, seasonal models, BT thresholds
- Bhatt et al, 2017 and 2019 developed channel-specific monthly empirical BRDFs
  - DCCs follow the sun and have a well described seasonal migration
  - SWIR bands impacted by cloud particle size and atmospheric absorption
  - reduced natural variability by up to 45% in Aqua-MODIS SWIR bands
  - 65% NPP-VIIRS SWIR bands based on PDF mean statistic

Current VIIRS DCC Methodology

- Data Used
  - For this study, NOAA-20 (N20) VIIRS NASA level 1B C2.1 pixel radiances , sub-sampled at every other scanline and pixel
- DCC pixels selection criteria
  - BT(11µm) < 205 K
  - Spatial Homogeneity $(H_{0.65}) < 3\%$
  - SDV (11µm) < 1 K
  - solar zenith angles (SZAs) and view zenith angles (VZAs) are limited to less than 40 degrees
  - tropical zone of $\pm 20°$ latitude
- BRDFs
  - Hu BRDF for the visible bands
  - Empirical monthly BRDFs for each SWIR band
- Stability monitoring statistics
  - Use the PDF mode for the visible bands
  - Use the mean statistic for SWIR bands

Annual and Monthly BRDF models

- Derived by partitioning the DCC-identified pixel *Radiance* (L') into angular bins defined by 5° SZA, 5° VZA, and 10° relative azimuth angle (RAA) intervals
- The reference angular condition chosen (SZA = 22.5°, VZA = 32.5°, RAA = 145°) represented the most frequently sampled angular conditions, ensuring robust statistical representation.

$$L_{corrected-annual} = L' x \frac{BRDF(22.5°,32.5°,145°,annual)}{BRDF(SZA,VZA,RAA,annual)}$$

$$L_{corrected-monthly} = L' x \frac{BRDF(22.5°,32.5°,145°,annual)}{BRDF(SZA,VZA,RAA,month)}$$

Where,

$L_{corrected-annual}$ = BRDF corrected radiances after applying annual BRDF

$L_{corrected-monthly}$ = BRDF corrected radiances after applying monthly BRDF

Comparison of various BRDF correction models for global domain

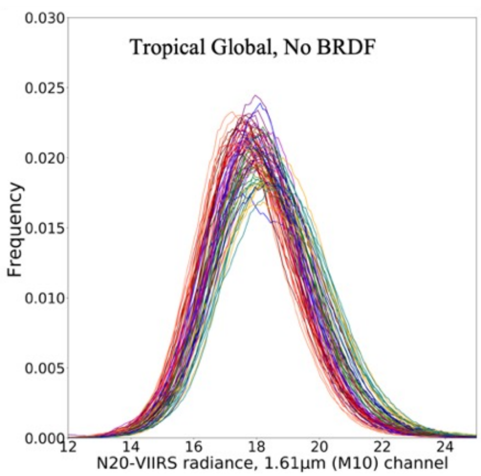

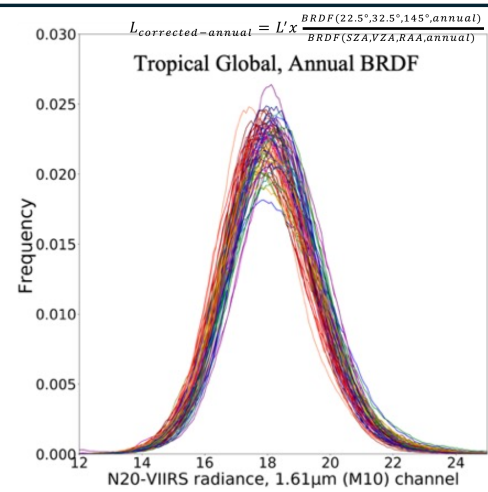

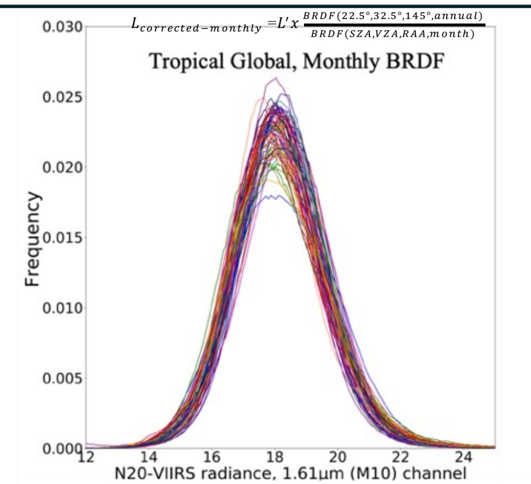

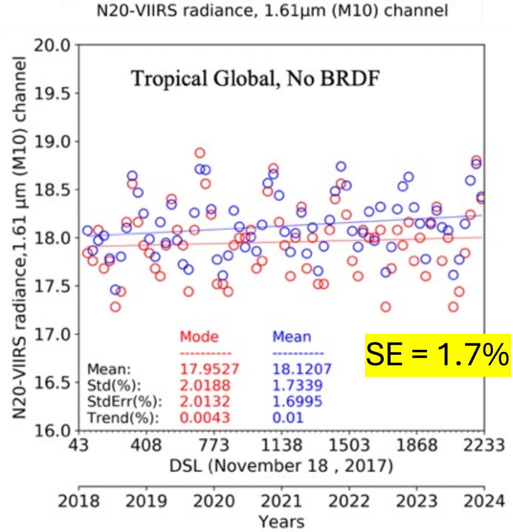

SE = 1.7%

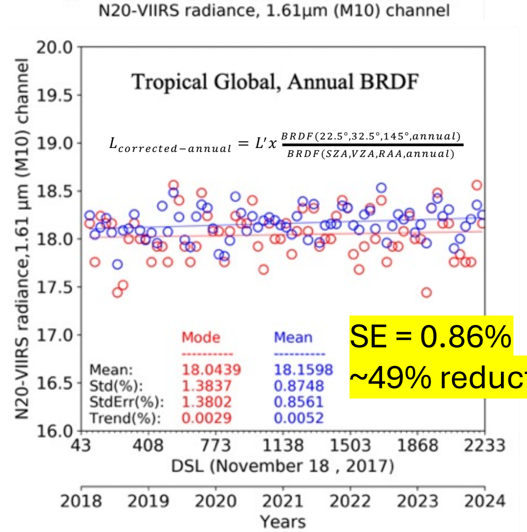

SE = 0.86%
~49% reduction

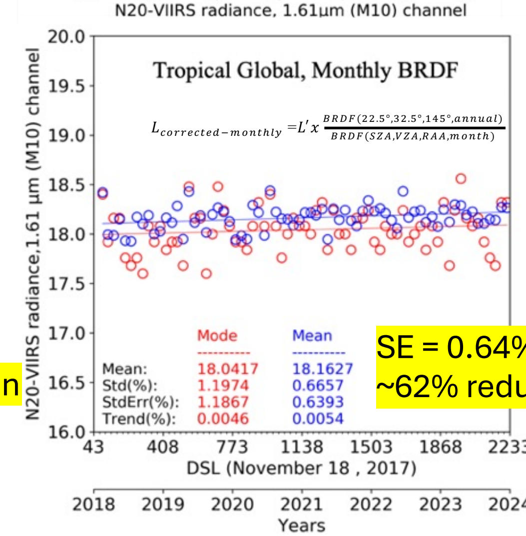

SE = 0.64%
~62% reduction

DCC over ocean vs DCC over land

- Land and Ocean have different microphysical properties
- The land DCC radiance response and intensity is greater over land than over oceans
- Ocean has wider convective cores; longer sustained updrafts
- Ocean has distinct day/night (greater intensity) variation in convective system
- L1B product provides a pixel surface type with each pixel
- Build a separate empirical land and ocean DCC BRDFs improve the overall stability of the DCC-IT methodology

Coverage	Surface	No of Pixels	Channel scaled radiance ($Wm^{-2}sr^{-1}\mu m^{-1}$)			
			1.24µm	**1.38µm**	**1.61µm**	**2.25µm**
Tropics	All	$104.1x10^6$	98.4	69.9	18.1	8.9
	Land	$27.5x10^6$	100.7	73.3	19.0	9.3
	Ocean	$75.7x10^6$	97.5	68.6	17.8	8.8
TWP	All	$42.5x10^6$	97.1	68.1	17.6	8.7
	Land	$4.7x10^6$	98.8	70.0	18.4	8.9
	Ocean	$37.9x10^6$	97.2	68.1	17.7	8.7

- **DCC over land is brighter than DCC over ocean (3.2%-6.9%)**
- **Need to take into account the land and ocean brightness difference when combining land and ocean DCC**

Land BRDF model normalized to ocean

$$L'_{corrected_{land}} = L'_{land} \ x \ \frac{BRDF_{ocean}(22.5°,32.5°,145°,annual)}{BRDF_{land}(SZA,VZA,RAA,month)}$$

$$L_{corrected_{ocean}} = L'_{ocean} \ x \ \frac{BRDF_{ocean}(22.5°,32.5°,145°,annual)}{BRDF_{ocean}(SZA,VZA,RAA,month)}$$

$$L_{corrected_{combined}} = L'_{corrected_{land}} + L_{corrected_{ocean}}$$

Where,

$L_{corrected_{land}}$ = BRDF corrected radiances after applying monthly land BRDF

$L_{corrected_{ocean}}$ = BRDF corrected radiances after applying monthly ocean BRDF.

For this approach we normalize land with ocean and ocean with ocean

Takes into account the brightness difference between land and ocean

Combined Land-only (normalized to ocean) and Ocean-only BRDF models

$L_{corrected_{ocean}}$ | $L'_{corrected_{land}}$ | $L'_{corrected_{land}} + L_{corrected_{ocean}}$

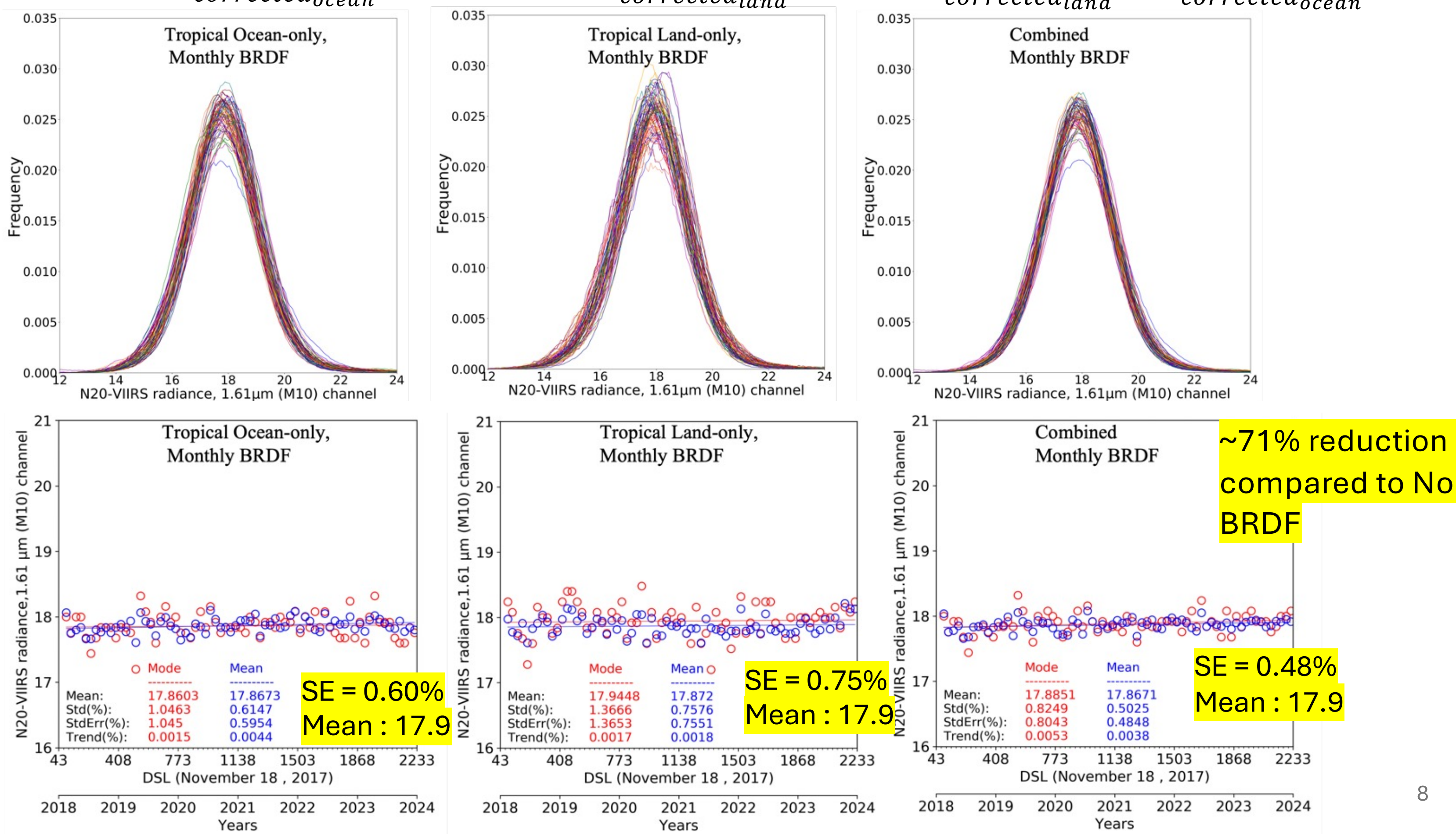

BRDF analysis in global domain

SN	Tropic surface	BRDF	Channel Mean Standard Error (%)			
			1.24µm (M8)	1.38µm (M9)	1.61µm (M10)	2.25µm (M11)
1	All	None	0.55	1.29	1.69	1.27
2	All	Annual All	0.47	1.10	0.85	0.70
3	All	Monthly All	0.30	0.71	0.63	0.50
4	Land-only	None	0.57	1.24	1.72	1.31
5	Land-only	Annual Land	0.50	1.08	1.29	1.03
6	Land-only	Monthly Land	0.30	0.72	0.75	0.60
7	Ocean-only	None	0.49	1.25	1.42	1.00
8	Ocean-only	Annual Ocean	0.47	1.15	0.77	0.60
9	Ocean-only	Monthly Ocean	0.27	0.69	0.59	0.43
10	Land + Ocean	Monthly Land (Land)* + Monthly Ocean	0.45	0.98	0.94	0.76
11	Land + Ocean	Monthly Land (Ocean)** + Monthy Ocean	0.24	0.62	0.48	0.37

*Land BRDFs are normalized by land pixels
**Land BRDFs are normalized by ocean pixels

- Monthly BRDFs outperform annual models, reducing temporal variation by up to 62% and effectively removing seasonal DCC radiance signatures compared with no BRDF application
- Combining land and ocean data after normalization achieves up to 26% additional trend SE reduction compared to the monthly BRDFs

Kernel Density Estimation(KDE) & PDF Statistics

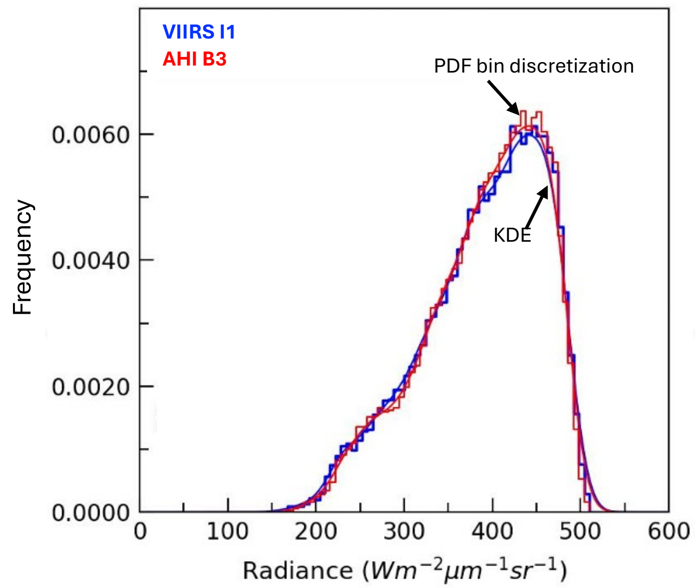

- The PDF shape is dependent on the radiance interval, which result in bin discretization,
- Kernel density estimation (KDE) from the gaussian_kde function

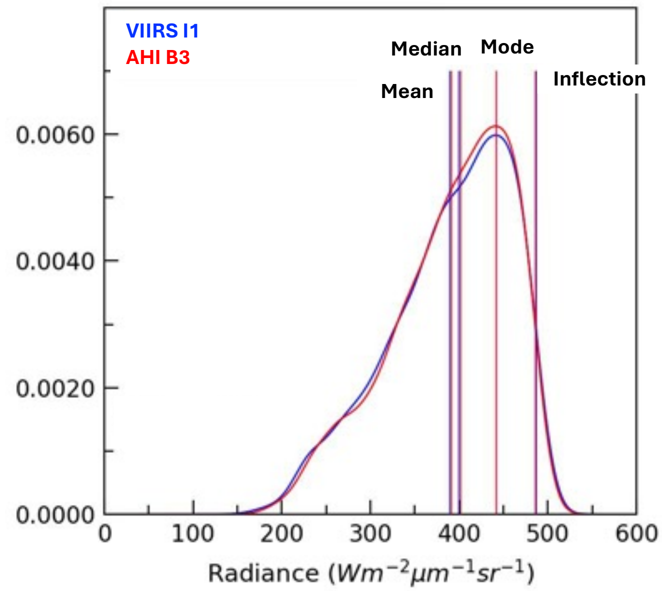

- **Mean** = average of the pixel radiances
- **Median** = radiance where half of the pixels are a lesser radiance and half of the pixels are higher radiance
- **Mode** = radiance with the greatest frequency
- **Inflection point** = radiance where the curvature sign changes (greater than mode and 10%*max frequency)

2019 monthly PDF histograms

M5 0.65μm N20 VIIRS

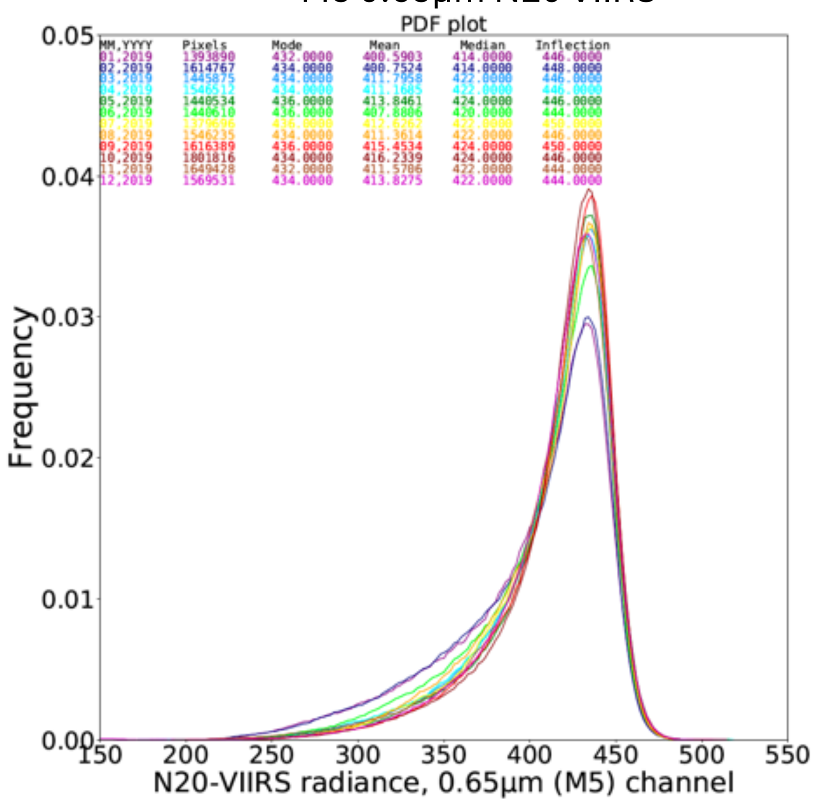

- The visible PDF shapes are consistent over the months

M10 1.61μm N20 VIIRS

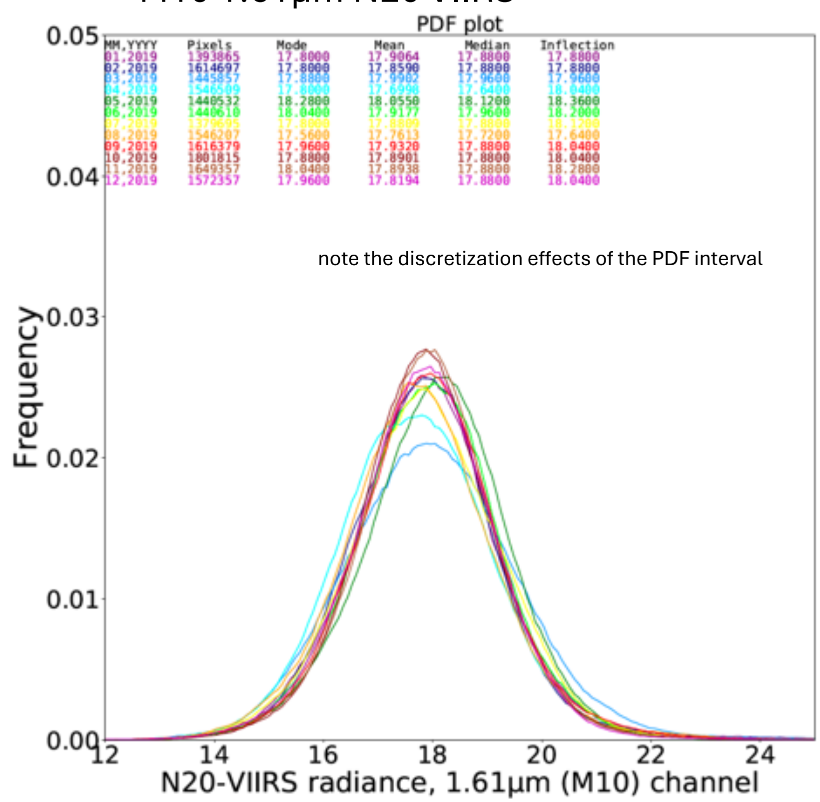

- The SWIR band PDF shapes vary considerably across month
- Either inadequate BRDF or missing DCC microphysical parameter

2019 monthly KDE histograms

M5 0.65µm N20 VIIRS

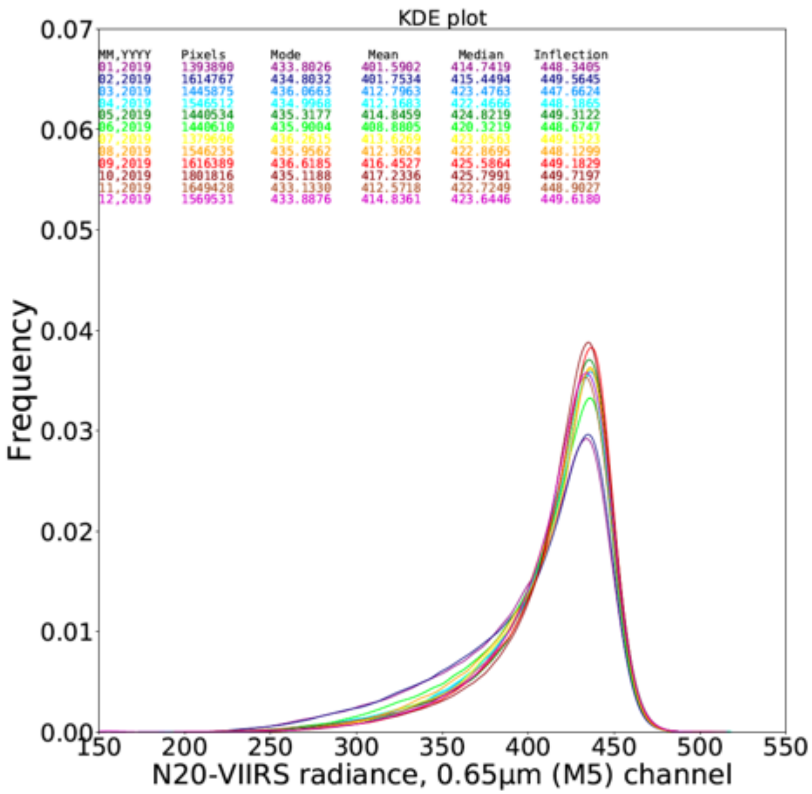

- The visible KDE shapes are consistent over the months
- The KDE statistics should be similar monthly

M10 1.61µm N20 VIIRS

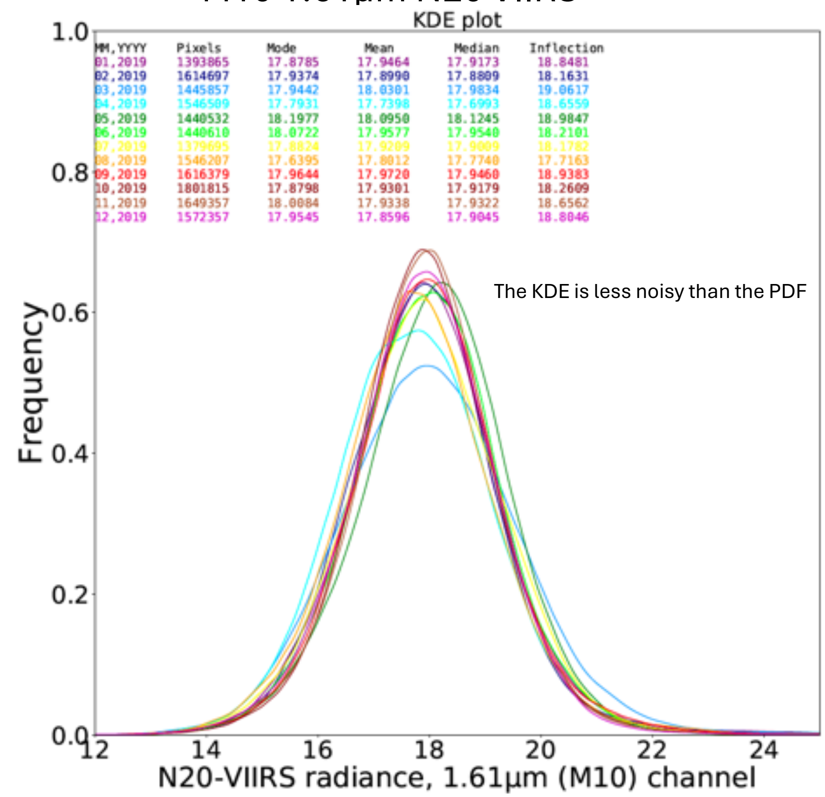

- The SWIR band PDF shapes vary considerably across month
- The KDE statistics will vary monthly

May yearly KDE histograms

M5 0.65µm N20 VIIRS

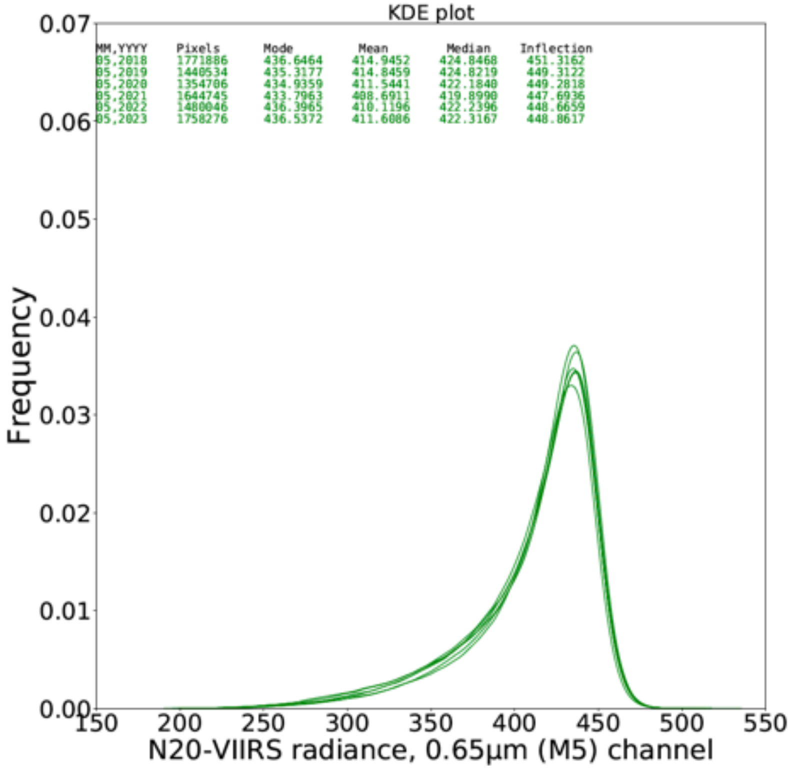

M10 1.61µm N20 VIIRS

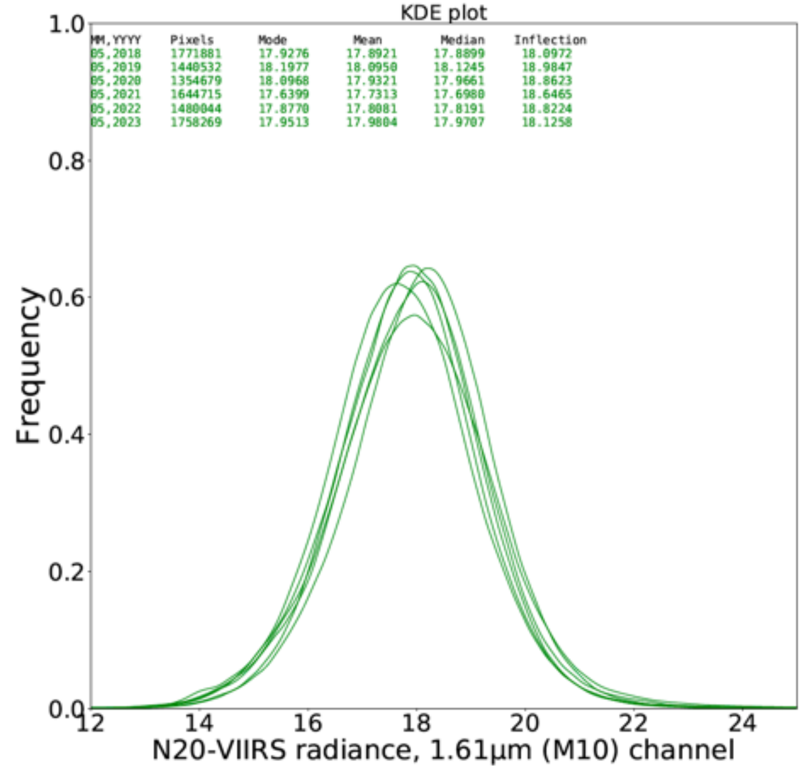

- The visible KDE shapes are consistent inter-annually

- The SWIR band KDE shapes vary inter-annually
- Deseasonalization will not be effective to reduce trend SE

M5 0.65 µm VIIRS stability

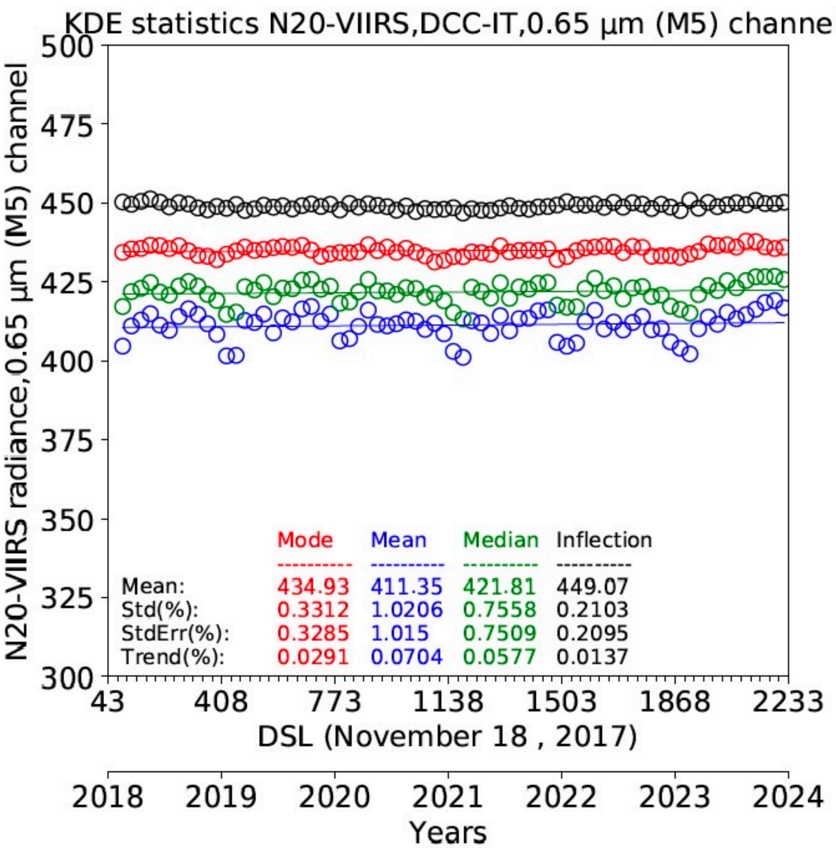

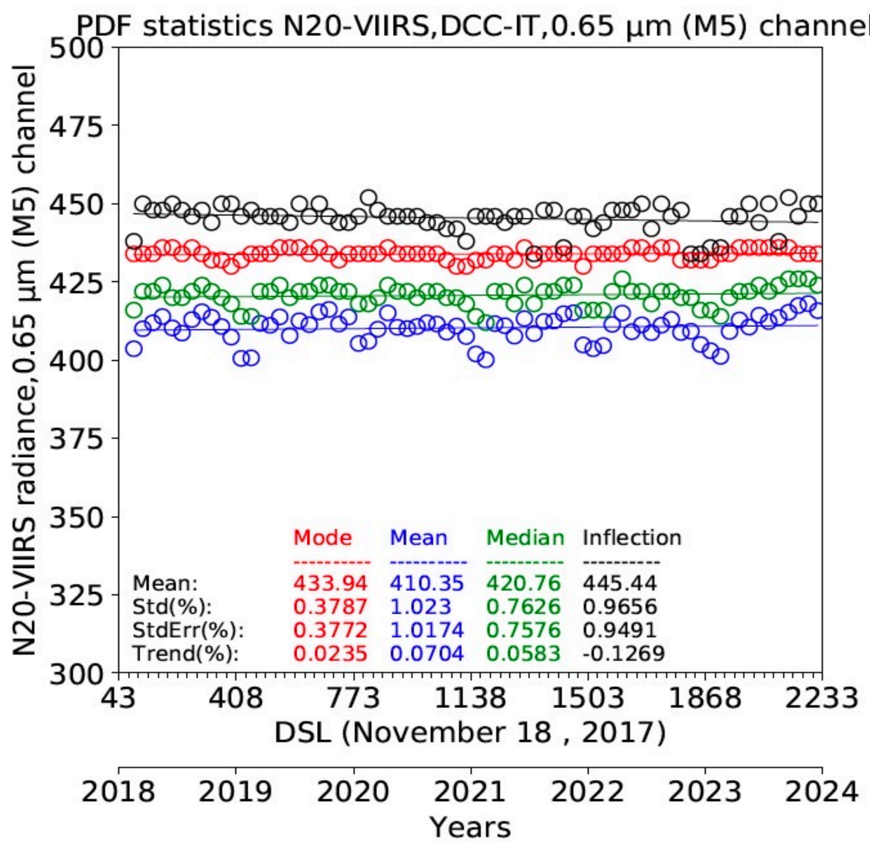

- For visible bands the KDE mode and inflection point are more stable than the PDF
- The KDE inflection point is the most stable KDE statistic

M10 1.61 µm VIIRS stability

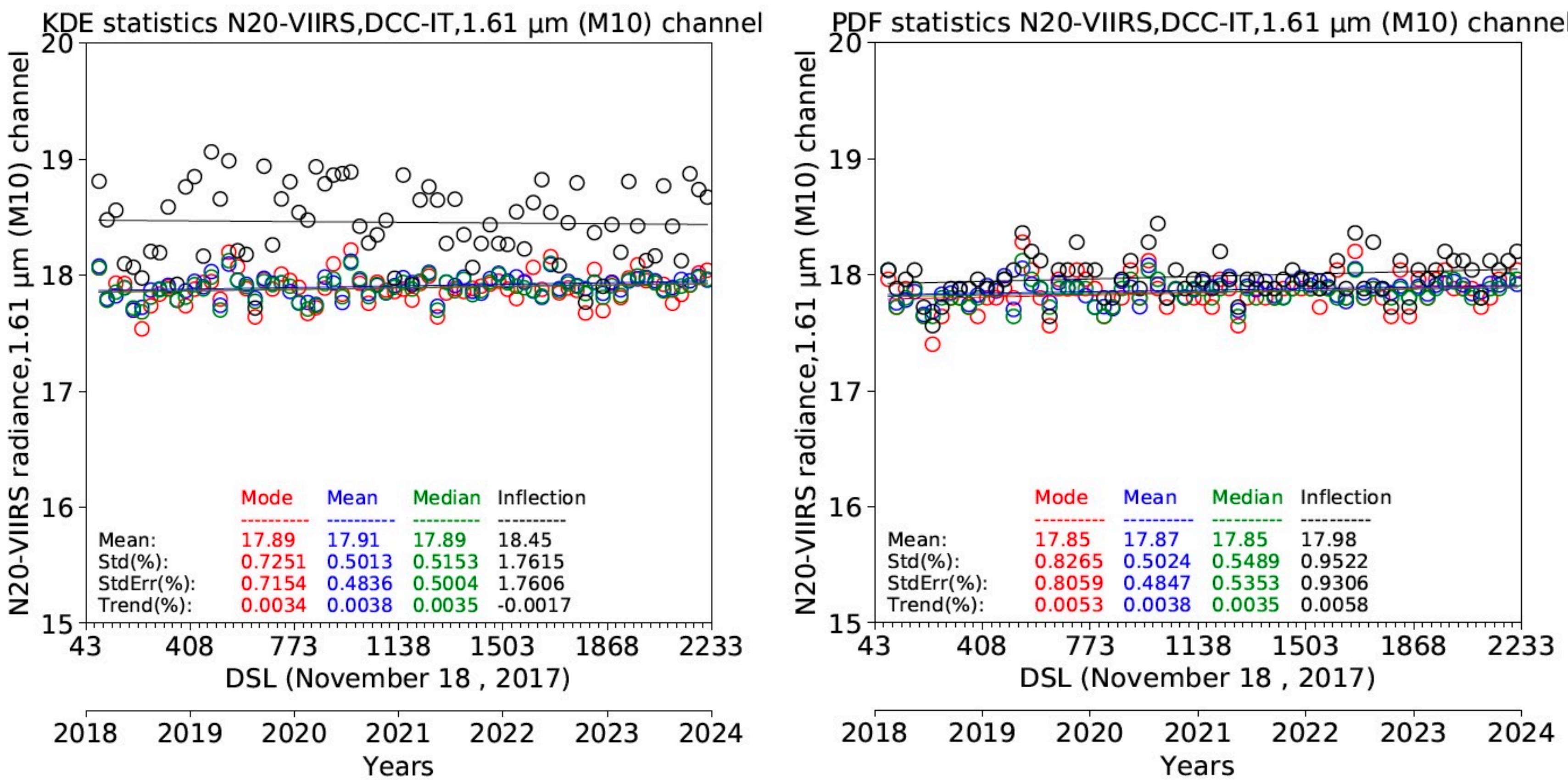

- For SWIR bands the mean, median, and mode have similar radiances
- The inflection point is difficult to pinpoint due to the PDF discretization, finds the first slope change, maybe try half maximum

Trend standard errors (%) by KDE/PDF statistics

N20-VIIRS channel	Standard error (%)							
	KDE mode	KDE mean	KDE median	KDE inflection	PDF mode	PDF mean	PDF median	PDF inflection
M3	0.40	1.00	0.77	**0.29**	0.48	1.00	0.77	1.06
M4	0.40	0.99	0.76	**0.33**	0.46	1.00	0.78	1.16
I01	0.39	1.01	0.77	**0.33**	0.39	1.02	0.78	1.09
M5	0.33	1.02	0.75	**0.21**	0.38	1.02	0.76	0.95
M7	0.23	0.93	0.58	**0.22**	0.28	0.93	0.60	0.79
M8	0.30	0.24	**0.23**	1.01	0.36	0.24	0.24	0.68
M9	0.99	0.62	**0.57**	2.21	1.10	0.63	0.56	1.20
I03	0.70	**0.48**	0.50	1.92	0.74	0.48	0.52	0.86
M10	0.72	**0.48**	0.50	1.76	0.81	0.48	0.54	0.93
M11	0.54	**0.38**	0.38	1.52	0.64	0.38	0.39	0.69

- Bold text indicates the lowest trend standard errors
- Mean and Median should not depend on either the PDF or KDE approach

Updated VIIRS DCC Methodology

- Data Used
  - NOAA-20 (N20) VIIRS level 1B pixel radiances , sub-sampled at every other scanline and pixel
- DCC pixels selection criteria (no change)
  - BT(11µm) < 205 K
  - Spatial Homogeneity $(H_{0.65}) < 3\%$
  - SDV (11µm) < 1 K
  - solar zenith angles (SZAs) and view zenith angles (VZAs) are limited to less than 40 degrees
  - tropical zone of $\pm 20°$ latitude
- BRDFs
  - Hu BRDF for the visible bands
  - Ocean and Land empirical monthly BRDFs for each SWIR band
- Stability monitoring statistics
  - Use KDE instead of PDF to construct histograms
    - Do not need to estimate histogram interval, the interval is optimized
    - Provides robust histograms for sparse DCC sampling, PDF shape is noisier
  - Use the KDE inflection for the visible bands
  - Use the mean statistic for SWIR bands, use median for some SW bands
    - There are still inter-annual variations for SWIR bands not resolved by the empirical BRDFs

Conclusions

- Monthly BRDFs outperform annual models, reducing temporal variation by up to 62% and effectively removing seasonal DCC radiance signatures compared with no BRDF application
- Applying separate ocean and land BRDFs achieves up to 26% additional trend SE reduction compared to the monthly BRDFs for SWIR bands
  - Must normalize the brighter land reflectances with the ocean reflectance
- The visible band PDF shapes are similar both monthly and inter-annually
- The SWIR band PDF shapes vary both monthly and inter-annually
- The kernal density estimation (KDE) to provide a PDF shape removes the discretization impact and performs under sparse sampling
- The KDE/PDF mean, median, mode, and inflection points were analyzed for imager stability assessments
  - Use the KDE inflection for the visible bands
  - Use the mean statistic for SWIR bands, use median for some SW bands
    - There are still inter-annual variations for SWIR bands not resolved by the empirical BRDFs